Lithosphere

Paleoseismologic evidence for multiple Holocene earthquakes on the Calico fault: Implications for earthquake clustering in the Eastern California shear zone

Plamen N. Ganev, James F. Dolan, Kimberly Blisniuk, Mike Oskin and Lewis A. Owen

Email alerting services	click www.gsapubs.org/cgi/alerts to receive free e-mail alerts when new articles cite this article
Subscribe	click www.gsapubs.org/subscriptions/ to subscribe to Lithosphere
Permission request	click http://www.geosociety.org/pubs/copyrt.htm#gsa to contact GSA

Notes

THE
GEOLOGICAL
SOCIETY
OF AMERICA

Paleoseismologic evidence for multiple Holocene earthquakes on the Calico fault: Implications for earthquake clustering in the Eastern California shear zone

Plamen N. Ganev[1],*, James F. Dolan[1], Kimberly Blisniuk[2], Mike Oskin[2], and Lewis A. Owen[3]

[1]DEPARTMENT OF EARTH SCIENCES, UNIVERSITY OF SOUTHERN CALIFORNIA, LOS ANGELES, CALIFORNIA 90089, USA
[2]DEPARTMENT OF GEOLOGY, UNIVERSITY OF CALIFORNIA–DAVIS, DAVIS, CALIFORNIA 95616, USA
[3]DEPARTMENT OF GEOLOGY, UNIVERSITY OF CINCINNATI, CINCINNATI, OHIO 45221, USA

ABSTRACT

Paleoseismologic data from trenches excavated across the Calico fault in the Eastern California shear zone reveal evidence for four surface ruptures during the past ~9000 yr. Twelve optically stimulated luminescence dates constrain the timing of these surface ruptures, which are defined by the geometry of growth strata, fissure fills, and upward fault terminations, to 0.6–2.0 ka, 5.0–5.6 ka, 5.6–6.1 (or possibly 7.3) ka, and 6.1 (or 7.3) to 8.4 ka. Geomorphologic mapping of the 8 km section of the fault extending southward from the trenches reveals two sets of displacements that record the slip from the past two or three surface ruptures. The slip caused by the most recent event was ~2.0 m, while the cumulative slip during the penultimate (and possibly the antepenultimate) event was ~4.5 m. The ages of the paleoearthquakes coincide with periods of clustered moment release identified previously on other faults in the Eastern California shear zone at 0–1.5 ka, 5–6 ka, and ca. 8–9.5 ka, with two Calico fault surface ruptures occurring during the 5–6 ka Eastern California shear zone cluster. These data strongly reinforce earlier suggestions that earthquake recurrence in the Eastern California shear zone is highly clustered in time and space. Such seismic clustering suggests that at least some regional fault networks undergo distinct periods of systemwide accelerated seismic moment release that may be driven by feedbacks between fault-loading rate and earthquake activity.

INTRODUCTION

There is a growing body of evidence that earthquakes cluster at a wide variety of spatial and temporal scales over both individual faults and regional fault networks (e.g., Ambraseys, 1971; Marco et al., 1996; Dolan and Wald, 1998; Rockwell et al., 2000; Friedrich et al., 2003; Dawson et al., 2003; Weldon et al., 2004; Dolan et al., 2007). Documentation of the temporal and spatial scales over which clustering occurs is important for developing tectonic models for accurate seismic hazard assessment (e.g., probabilistic seismic hazard analysis [PSHA]). Moreover, an understanding of the mechanisms for clustering would contribute to a deeper understanding of earthquake physics and the geodynamics of the lithosphere.

The Calico-Blackwater fault system is the longest in the Mojave section of the Eastern California shear zone, a set of predominantly north- to northwest-striking dextral faults that trends northward from the San Andreas fault, across the Mojave Desert, and to the east of the Sierra Nevada (Fig. 1). Recent studies indicate a long-term slip rate for the Calico fault of 1.8 ± 0.3 mm/yr, averaged over the past 57 ± 9 k.y. (Oskin et al., 2007, 2008). Although this represents approximately one third of the total geologic slip rate across the six major faults (i.e., Helendale, Lenwood, Camp Rock, Calico-Blackwater, Pisgah, and Ludlow) that comprise the Mojave section of the Eastern California shear zone, the paleoearthquake history of the Calico fault has not previously been documented.

A compilation of paleoseismologic data from the majority of the faults in the Mojave section of the Eastern California shear zone (but not including

the Calico fault) revealed that strain release has been highly episodic over the past 12,000 yr, with pronounced clusters of earthquakes at ca. 8–9.5 ka, 5–6 ka, and during the past ~1000–1500 yr (Rockwell et al., 2000). The 1992 M_w 7.3 Landers and 1999 M_w 7.1 Hector Mine earthquakes are the two most recent earthquakes of the ongoing, latest Holocene cluster.

The lack of previous paleoseismic studies of the Calico fault thus leads to a simple test of the clustering hypothesis. Because the Calico fault slips faster than other nearby faults, larger or more frequent earthquakes should accommodate its slip. If regional clustering of earthquakes modulates fault-zone activity in the Mojave Desert section of the Eastern California shear zone, then these earthquakes should fall into the regional clustering time periods identified by Rockwell et al. (2000). In this paper, we describe the results of a paleoseismologic trench study and geomorphic analysis of offset features along the northern part of the Calico fault, and discuss the implications of our results for earthquake behavior and seismic hazard assessment.

SITE DESCRIPTION

Our study site is located in the town of Newberry Springs, California, ~30 km east of the city of Barstow (Figs. 1–3). The ~N30°W-striking fault trace at the site is well expressed on aerial photographs as a very low-relief (<15–20 cm high), predominantly east-facing scarp and a pronounced vegetation lineament that extend across the playa deposits (Fig. 2). Two parallel fault strands, a prominent eastern strand and a more subtle western strand, are recognizable on the surface. The sediment sources are alluvial fans to the west of the site originating from the Newberry Mountains.

*Corresponding author: 3651 Trousdale Parkway, Los Angeles, CA 90089; ganev@usc.edu, +1-213-740-8208.
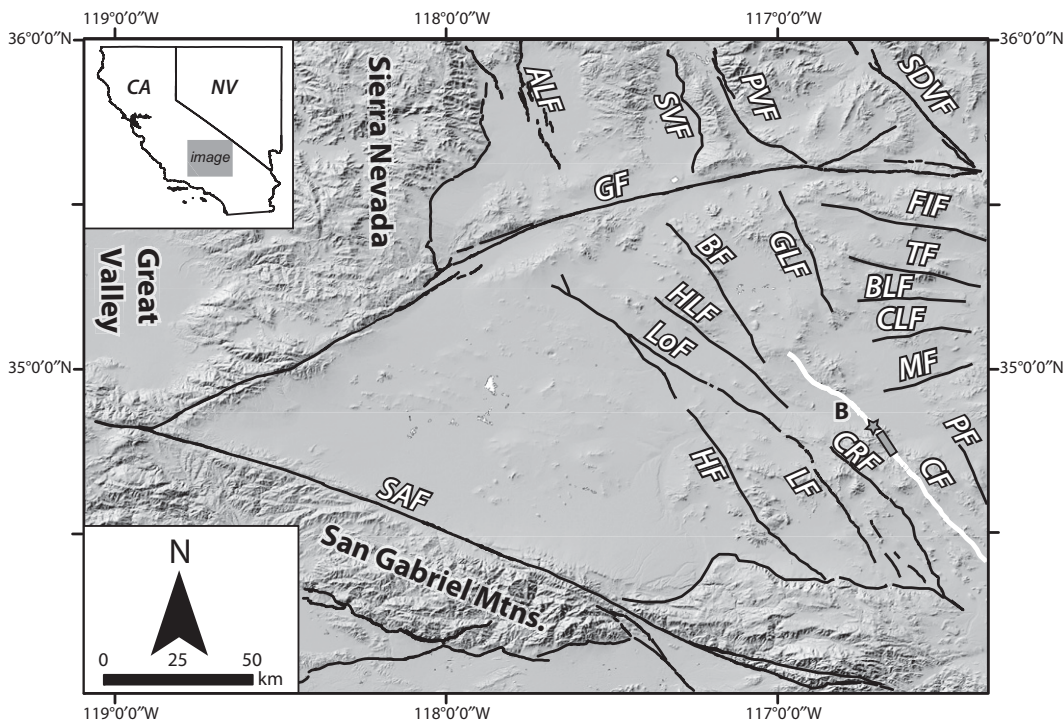
Figure 1. Map showing the faults of the Eastern California shear zone in the Mojave Desert. The Calico fault is highlighted in white, gray star indicates the location of the trench sites, and the gray quadrangle shows our geomorphic survey area. ALF—Airport Lake fault, B—Barstow, BF—Blackwater fault, BLF—Bicycle Lake fault, CF—Calico fault, CLF—Coyote Lake fault, CRF—Camp Rock fault, FIF—Fort Irwin fault, GF—Garlock fault, GLF—Goldstone Lake fault, HF—Helendale fault, HLF—Harper Lake fault, LF—Lenwood fault, LoF—Lockhart fault, MF—Manix fault, PF—Pisgah fault, PVF—Panamint Valley fault, SAF—San Andreas fault, SDVF—southern Death Valley fault, TF—Tiefort Mountain fault.
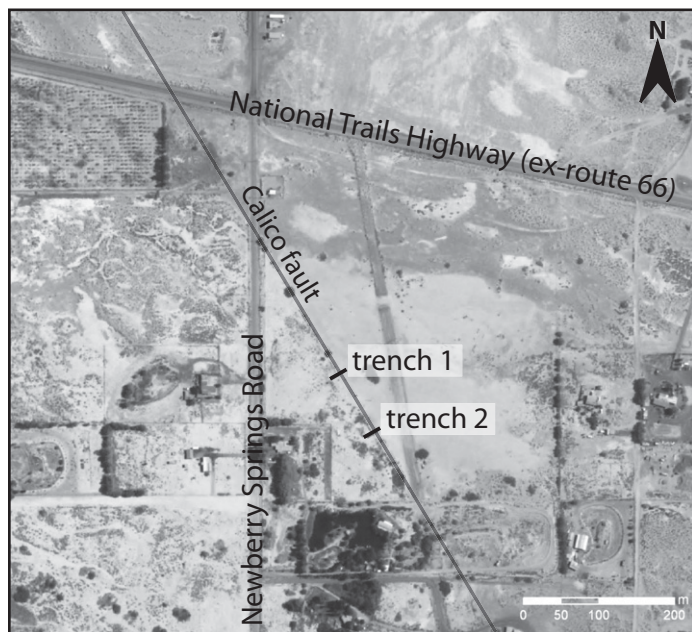
Figure 2. Aerial photograph showing the surface expression of the Calico fault (National Agriculture Imagery Program, 2005). The gray line indicates the mappable fault trace, which creates a vegetation lineament with sparse vegetation to the northeast. The trench site is located on playa sediments to the northeast of the Newberry Mountains. The photograph in Figure 3 is taken from the overpass at Newberry Springs Road and National Trails Highway.
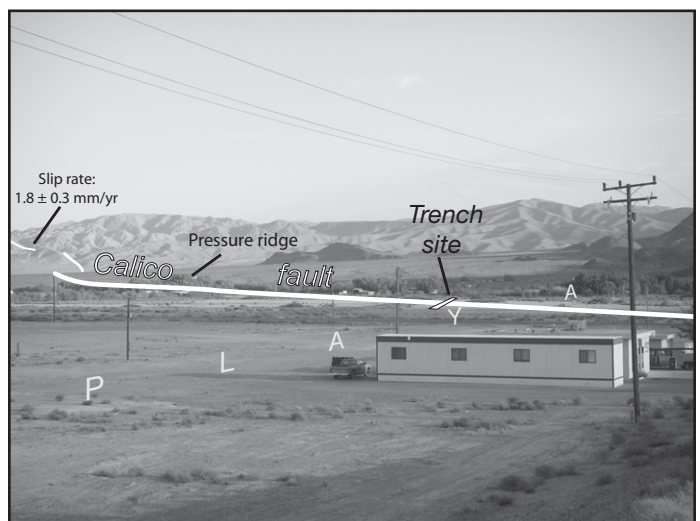
Figure 3. View southeastward toward the playa trench site. The Calico fault trace is shown in white. Shown in the distance is the location of Oskin et al.'s (2007) Pleistocene slip-rate study.

PALEOSEISMIC TRENCHING

We excavated two fault-perpendicular trenches in the playa where the fault trace was well expressed and where no vegetation was present to obstruct the excavation, or to disturb the youngest strata. The northern trench was 30 m long and 0.9 m wide, with a maximum depth of 3 m. The trench end points were located at 34°49.190′N, 116°39.697′W, and 34°49.182′N, 116°39.715′W. The length of the trench ensured that all fault strands were exposed. A second trench (the "southern trench") was excavated ~100 m to the south in order to assess the repeatability of the event chronology logged from the northern trench. The southern trench was 15 m long and 3.5 m deep. The western 11 m of this trench were 0.9 m wide, whereas the 3 m east of the main fault zone were 1.4 m wide due to wall-stability problems. The end points of this trench were located at 34°49.138′N, 116°39.668′W, and 34°49.132′N, 116°39.675′W.

Both trenches exposed fluvial, lacustrine, and playa sediments consisting of well-stratified and thinly bedded pebble gravel to coarse-grained sand, silt, and clay, respectively (Fig. 4). The fault zone exposed in the trenches consists of two strands—the eastern (main) strand and a less-pronounced western strand (Fig. 5). Although motion on the two strands is predominantly strike slip, subordinate vertical components of movement have created a down-dropped block between them. Total vertical separation across the eastern fault at the base of the northern trench is ≥2.5 m, and episodic thickening of growth strata across these faults into the central structural trough helped us to determine the rupture history of the fault. Both the eastern and western fault strands are exposed in the northern trench, but only the main, eastern strand of the fault and the eastern half of the interfault trough are exposed in the southern trench. Major stratigraphic units are numbered in increments of 10, increasing with depth, whereas subunits are labeled using a combination of the respective major stratigraphic unit number plus an alphabetical letter, descending with depth. For example, unit 90 is a pale yellowish-brown coarse-grained sand and gravel, whereas subunit 90A is a fine-grained layer that makes up the uppermost part of unit 90. Detailed descriptions of the stratigraphic units are included in the GSA Data Repository.[1]

AGE CONTROL

One of the reasons we originally chose the study site was that playas tend to concentrate charcoal suitable for radiocarbon dating (the low-density charcoal fragments stay in suspension until deposited with the last remaining water to be evaporated on the playa). Unfortunately, we were unable to find charcoal in any of the deposits exposed in the trenches, despite intensive efforts to isolate even small quantities through "floating" the low-density charcoal in settling tubes. Fortunately, however, the sediments at the site were well suited to optically stimulated luminescence (OSL) dating, which is used to determine the time that has elapsed since a sediment sample was last exposed to daylight (Table 1) (Aitken, 1998). This technique has been successfully applied to dating deformed sediments from paleoseismic studies in the western United States (e.g., Machette et al., 1992; Crone et al., 1997; Rockwell et al., 2000; Lee et al., 2001; Kent et al., 2005; Wesnousky et al., 2005) and elsewhere in the world (e.g., Owen et al., 1999; Washburn et al., 2001; Wallinga, 2002; Rockwell et al., 2009). We dated 12 samples using OSL methods. At least two samples were dated from each of the layers bounding each of the event horizons in order

to replicate the ages. The sediment samples were collected by pounding 5-cm-diameter, 46-cm-long steel pipes with capped outer ends into the trench wall. The samples remained sealed in their tubes until processing in the safe-light conditions in the Luminescence Dating Laboratory at the University of Cincinnati. Sediment from at least 3 cm from both ends of the tube was removed, and the rest was dried in an oven at ~90 °C. Approximately 20 g of the dried sediment were ground to a fine powder and sent to the U.S. Geological Survey (USGS) Reactor in Denver for instrumental neutron activation analysis (INAA) to determine the concentration of radioisotopes for dose-rate determination.

The ages of our samples range from 0.6 ka to 8.4 ka, indicating that deposition of all of the strata exposed in the trenches occurred during Holocene time (Fig. 6; Table 1). The oldest sample (081407A) was collected from the southern wall of the southern trench, whereas the rest of our samples came from the southern wall of the northern trench (Table 1). Although the OSL ages indicate that the sediment accumulation rate has averaged ~0.4 mm/yr over the past 8.4 k.y., the rate has varied significantly over that time (Fig. 7). For example, between ca. 5.6 ka and ca. 5.0 ka, the rate of sediment accumulation increased to ~2 mm/yr, but subsequently decreased to ~0.2 mm/yr between ca. 5.0 ka and the present.

INTERPRETATION OF PALEO–SURFACE RUPTURES

The trench exposures revealed evidence for four Holocene surface ruptures on the Calico fault. We refer to these as events 1 (youngest) through 4 (oldest). The three most recent events are well expressed in the northern trench, whereas evidence for the oldest event is present only in the southern trench, in which we exposed deeper stratigraphy. As described in detail next, evidence for these paleoearthquake event horizons includes fissure fills, the geometry of growth strata (e.g., onlap of fault scarps), and upward fault terminations.

Event 1

Event 1 is best expressed in the northern trench, where it is recorded by the geometry of growth strata and upward fault terminations within unit 30, a dense pinkish-brown clay layer. The best evidence for this surface rupture comes from thickening of unit 30 into the central trough across both the main (eastern) and western fault zones (Fig. 5; Figs. DR1 and DR2 [see footnote 1]). Specifically, unit 30 increases in thickness across the western fault strand from ~10 cm west of the fault to 30–40 cm in the center of the northern trench. Unit 30 includes two subunits: unit 30A, a denser, more indurated clay, overlies unit 30B, which is slightly more friable. Unit 30B was most clearly defined on the southern wall of the northern trench, extending from meter 8, where it is fault contact with the uplifted older units to the east, across the midtrench trough to the western extent of the trench.

Unit 30B exhibits a relatively constant thickness of 10–15 cm, particularly west of meter 16. In contrast, unit 30A is restricted to the midbasin trough and onlaps unit 30B at meter 10 and meter 22 (Fig. 4). At meter 8, two strands of the main fault offset subunit 30B, but do not cut overlying unit 10. The eastern of these two strands juxtaposes unit 30B against unit 70 clay exposed in the uplifted block east of the main fault strand. Ten centimeters to the west, the second strand exhibits a 10-cm-high, east-side-up vertical separation of the lower part of subunit 30B.

Unit 30 thins markedly westward at the location of the western fault at meter 21.5. The exact stratigraphic level of the upward termination of this oblique reverse fault exposed is not clear; the fault cuts all strata below unit 40, but it cannot be traced confidently upward through the unit 40 soil overprint or into unit 30. However, the relatively constant thickness of
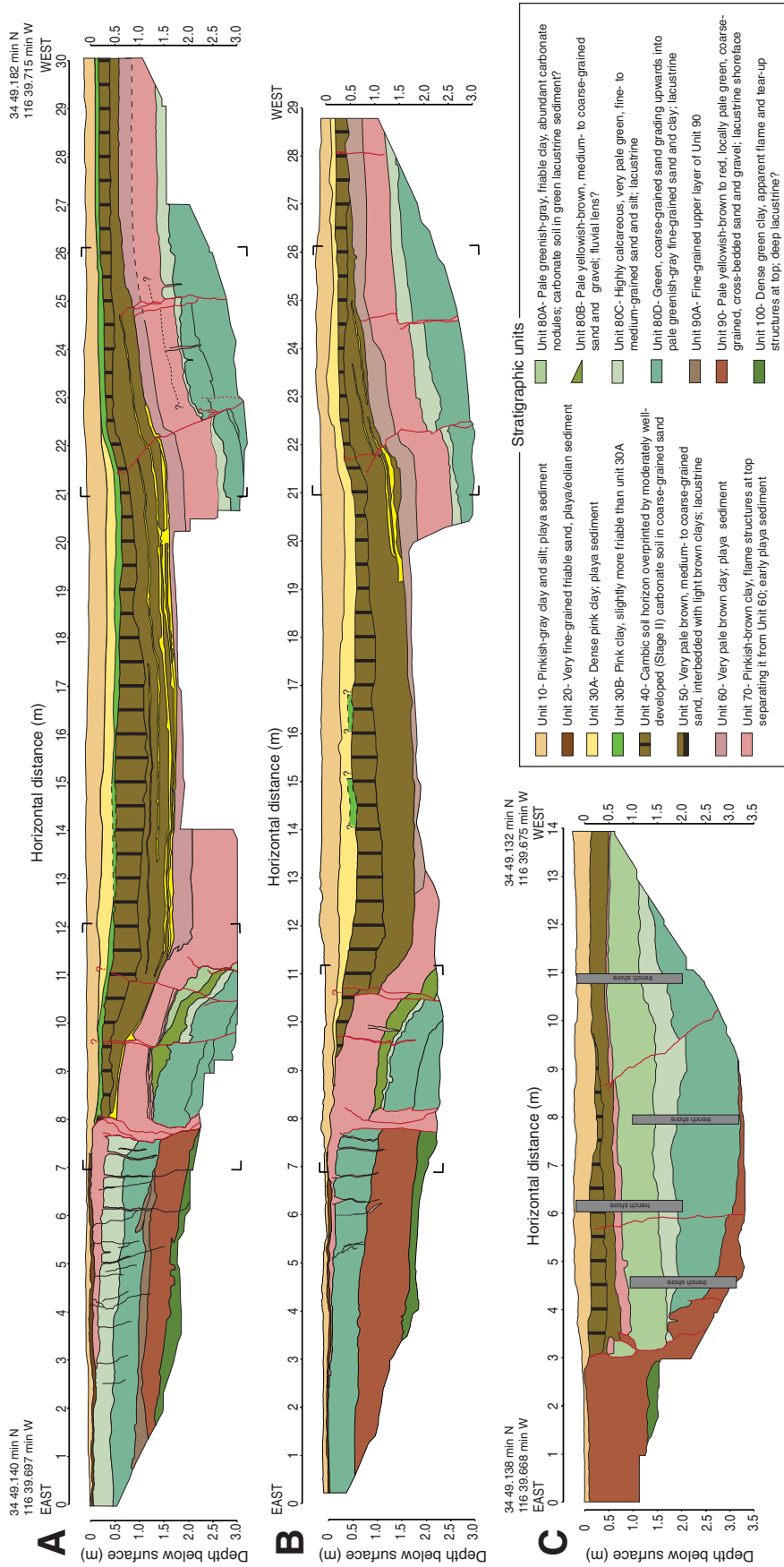
Figure 4. Simplified fault trench logs of the southern wall (A) and reversed northern wall (B) of the northern trench, and southern (C) wall of the southern trench show the general structure and stratigraphy of the trenches. Locations of Figures 5A (between meters 7–12 on the southern wall of the northern trench) and 5B (between meters 21–26 on the southern wall of the northern trench) and Figures DR1A (between meters 7–11 on the northern wall of the northern trench) and DR1B (between meters 21–26 on the northern wall of the northern trench) are outlined by black corners on logs A and B.
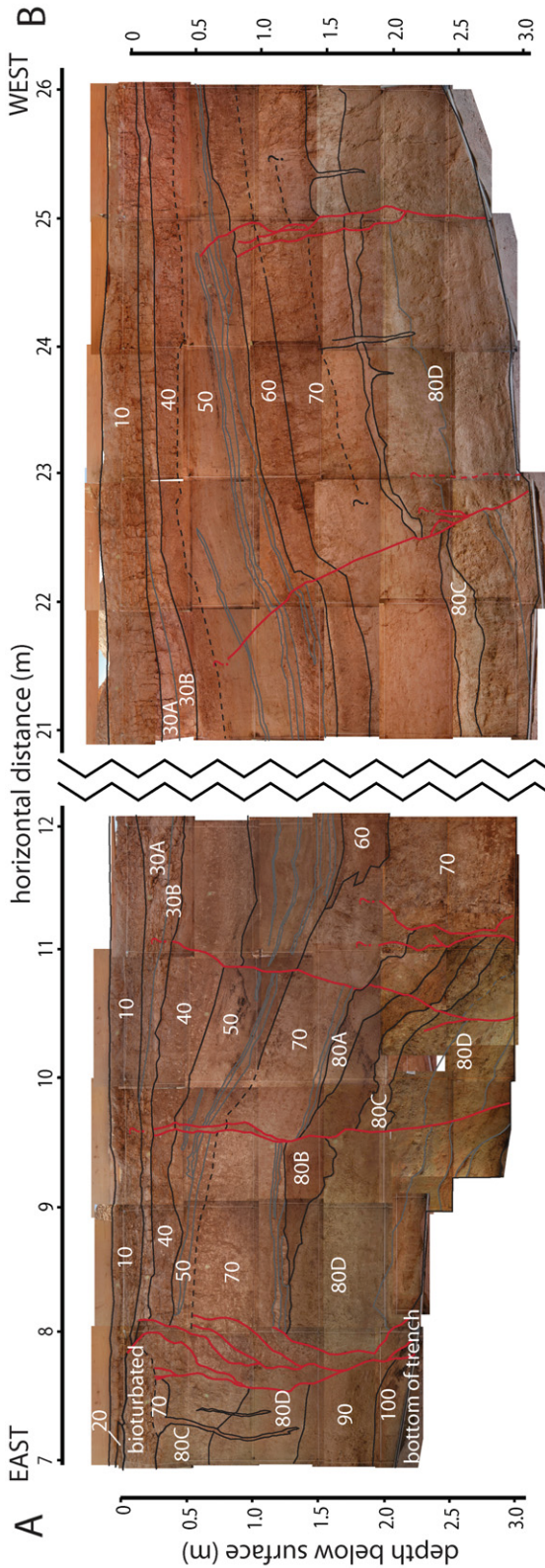
Figure 5. Detailed photograph logs between meters 7–12 and meters 21–26 from the southern wall of the northern trench. (A) Photograph log of the main (eastern) fault strand (visible between meters 7 and 8). Vertical separation is ~1 m with younger units, 30–50, buttressing against the scarp of unit 70. The vertical separation, along with fissure fills to the east of the eastern fault strand, provides evidence for event 3. Upward rupture terminations between meter 9 and meter 11 provide evidence for the most recent event. **(B)** Detailed photograph log between meters 21 and meters 26. The upward rupture terminations may be related to the penultimate event; however, it is difficult to discern their upward extent, and thus they may be due to the most recent surface rupture. A fissure fill within unit 70 at meter 24 provides evidence in support of event 3.

TABLE 1. SUMMARY OF OSL DATING RESULTS EXTRACTED FROM SEDIMENT, SAMPLE LOCATIONS, RADIOISOTOPE CONCENTRATIONS, MOISTURE CONTENTS, TOTAL DOSE RATES, D_E ESTIMATES, AND OPTICAL AGES

Sample number	Laboratory number	Location Latitude (°N)	Longitude (°W)	Altitude (masl)	Depth (cm)	Particle size (µm)	U* (ppm)	Th* (ppm)	K* (%)	Rb* (ppm)	Cosmic[†,§] (G/k.y.)	Dose rate[†,#] (G/k.y.)	n**	Mean equivalent dose[††] (Gy)	OSL age[§§] (ka)
051707B	DOLAN5	34.820	116.7	565	40	90–125	4.07	10.30	2.50	120.00	0.22 ± 0.02	3.92 ± 0.24	14	19.1 ± 0.8	1.1 ± 0.1
051707I	DOLAN12	34.820	116.7	565	80	75–150	4.81	8.25	2.88	114.00	0.21 ± 0.02	4.26 ± 0.26	35	14.3 ± 0.1	3.4 ± 0.2
051707J	DOLAN11	34.820	116.7	565	40	90–125	4.48	10.70	2.58	108.00	0.22 ± 0.02	4.10 ± 0.25	19	2.5 ± 22.5	0.6 ± 0.1
081407A	DOLAN7	34.820	116.7	565	300	90–125	1.38	7.03	3.62	138.00	0.16 ± 0.02	4.01 ± 0.29	8	33.8 ± 1.3	8.4 ± 0.7
081507A	DOLAN4	34.820	116.7	565	80	125–180	3.65	9.02	2.87	116.00	0.21 ± 0.02	4.05 ± 0.26	70	8.2 ± 0.2	2.0 ± 0.1
081507B	DOLAN1	34.820	116.7	565	170	90–125	4.10	13.00	2.46	135.00	0.19 ± 0.02	4.04 ± 0.24	40	22.7 ± 0.6	5.6 ± 0.4
081507C	DOLAN8	34.820	116.7	565	130	125–180	5.01	9.86	1.84	105.00	0.20 ± 0.01	3.51 ± 0.20	14	19.1 ± 0.8	5.4 ± 0.4
081507D	DOLAN3	34.820	116.7	565	240	90–125	3.05	8.07	1.71	89.30	0.17 ± 0.01	2.83 ± 0.17	44	20.6 ± 0.4	7.3 ± 0.5
081507E	DOLAN9	34.820	116.7	565	180	125–180	3.27	8.74	1.79	98.10	0.19 ± 0.01	3.00 ± 0.18	34	18.3 ± 0.7	6.1 ± 0.4
081507F	DOLAN10	34.820	116.7	565	170	125–180	1.14	3.86	3.21	111.00	0.19 ± 0.02	3.43 ± 0.25	35	19.2 ± 0.6	5.6 ± 0.4
081507G	DOLAN6	34.820	116.7	565	170	125–180	2.05	4.38	2.83	99.50	0.19 ± 0.02	3.34 ± 0.23	32	16.6 ± 0.5	5.0 ± 0.4
081507H	DOLAN2	34.820	116.7	565	70	125–180	2.64	5.93	3.12	112.00	0.21 ± 0.02	3.84 ± 0.26	40	19.0 ± 0.4	5.0 ± 0.4

Note: The location of the samples is 34.820°N, 116.662°W. OSL—optically stimulated luminescence; masl—meters above sea level.
*Elemental concentrations from instrumental neutron activation analysis of whole sediment measured at U.S. Geological Survey Nuclear Reactor Facility in Denver. Uncertainty was taken as ±10%.
[†]Estimated fractional water content was taken as 10% ± 5%.
[§]Estimated contribution to dose rate from cosmic rays calculated according to Prescott and Hutton (1994). Uncertainty was taken as ±10%.
[#]Total dose rate from beta, gamma, and cosmic components. Beta attenuation factors for U, Th, and K compositions incorporate grain-size factors from Mejdahl (1979). Beta attenuation factor for Rb was arbitrarily taken as 0.75 (cf. Adamiec and Aitken, 1998). Factors utilized to convert elemental concentrations to beta and gamma dose rates are from Adamiec and Aitken (1998), and beta and gamma components are attenuated for moisture content.
**Number of replicated equivalent dose (D_E) estimates used to calculate mean D_E. These are based on recuperation error of <10%.
[††]Weighted mean equivalent dose (D_E) determined from replicated single-aliquot regenerative-dose (SAR; Murray and Wintle, 2000) runs. Errors include an error from beta source estimated at about ±5%.
[§§]Errors incorporate dose rates errors and weighted errors of D_E.
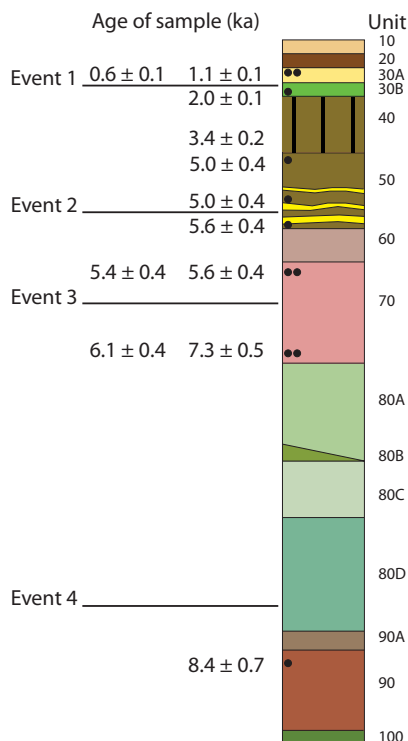
Figure 6. Composite stratigraphic column of playa units derived from both trenches. Black circles are depth locations of dated optically stimulated luminescence (OSL) samples with the respective ages on the left. Determined stratigraphic positions of event horizons are also labeled on the left. Descriptions of each unit are provided in Figure 4.
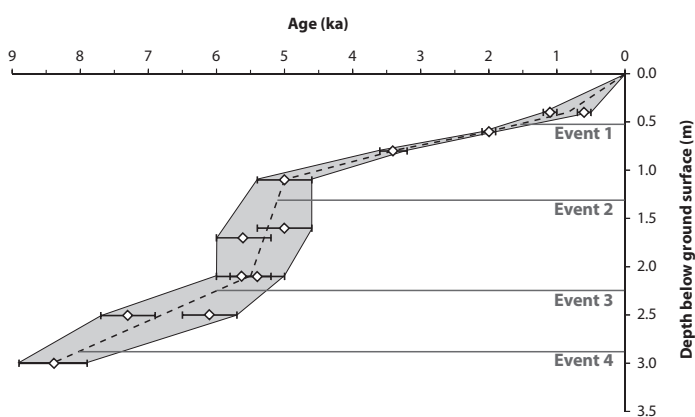
Figure 7. Sediment accumulation rate curve showing distributions of optically stimulated luminescence dates with depth below the surface (measured at meter 21 on the south wall of the northern trench for consistency). Uncertainty incorporates all random and systematic errors, including dose rates errors and weighted average uncertainty. The dashed line represents the best estimates of the sample ages, providing the sediment accumulation rate. The gray polygon represents the error envelope on the sedimentation rate. Depths of event horizons are shown at meter 21 from the north wall of the northern trench.

subunit 30B from meter 16 to the west end of the trench across this feature argues that subunit 30B was deposited on a near-horizontal surface and has subsequently been folded by slip on the thrust fault. Subunit 30B is composed of playa clay, and such fine-grained strata can drape significant scarps, but even clay units would likely exhibit some thickening across such a pronounced topographic scarp if it had existed prior to deposition of subunit 30B. Taken together, these stratigraphic and structural observations indicate that the most recent surface rupture at the trench site occurred after deposition of subunit 30B and before deposition of subunit 30A, which is interpreted to have largely filled in the postevent structural trough created during event 1.

Thickening of unit 30 into the midtrench trough records sedimentary growth of at least 20–30 cm following event 1. However, the top of unit 30 adjacent to the western fault is not flat, suggesting that growth of unit 30A did not completely fill the trough to its pre-event, horizontal playa surface, leaving a subtle (~10 cm high on southern wall, ~30 cm high on northern wall) east-facing scarp. This remaining subtle event 1 scarp was subsequently completely buried during deposition of unit 10, which extends up to the current near-horizontal playa surface. Thus, total vertical separation in event 1 across both strands is probably at least ~30 cm, and possibly more than 60 cm.

OSL sample 081507A from subunit 30B and samples 051707J and 051707B from subunit 30A constrain the age of event 1. The lower sample yielded an age of 2.0 ± 0.1 ka, whereas the upper samples yielded ages of 0.6 ± 0.1 ka and 1.1 ± 0.1 ka, respectively. Thus, the most recent surface rupture at the trench site occurred after 2.0 ± 0.1 and before 0.6 ± 0.1 (or 1.1 ± 0.1) ka. We note, however, that if there was any undetected partial bleaching of these (very young) samples, this would result in ages that are slightly too old. Whereas the general reproducibility of the ages of the other sample pairs from deeper in the section argues that partial bleaching is not a major problem in the trench, the ~500 yr difference in the ages of samples 051707J and 051707B, which were collected from the same stratigraphic level only 30 cm from each other, suggests that there may be some minor partial bleaching in some samples. Although we suspect that this effect is relatively minor, it would be most pronounced in the youngest samples. Thus, the OSL ages constraining event 1 should probably be considered maxima.

The upward terminations of the secondary fault strands exposed at meter 9.5 and meter 11 require additional discussion. Both of these faults clearly extend upward to at least the top of unit 40, but they cannot be traced confidently upward into unit 30B. We suspect that this is because the shallowest few tens of centimeters of the trench exposures encompassing units 10–30 exhibited pervasive, irregular cracking. This cracking does not appear to be tectonic in origin, but rather is related to development of a weak, blocky soil texture in these units. Thus, although the stratigraphic contacts in this section could be mapped in detail, the exact upward terminations of the faults could not be unequivocally distinguished from nontectonic cracking within the lower part of unit 30. The possibility that the faults at meter 9.5 and meter 11 do terminate upward at the base of unit 30B suggests the possibility of another event horizon at this stratigraphic level.

If these upward fault terminations do record an additional, pre–event 1 surface rupture, this event must have occurred before deposition of unit 30B at 2.0 ka, and after the 3.4 ka age of unit 40. The 3.4 ka OSL date from unit 40, however, dates the deposition of this unit, and these sediments must have been exposed at the ground surface for a significant period of time prior to deposition of subunit 30B, as evidenced by the presence of the cambic and carbonate soils that developed within unit 40, but which are not evident in unit 30. The observation that the faults at meter 9.5 and meter 11 are clearly discernible to the top of unit 40, through the cambic

and carbonate soil overprints, indicates that these faults must have ruptured after most, or all, pedogenesis in unit 40. Thus, if the poorly defined upward terminations of these faults do record a distinct event horizon, this earthquake must have occurred just before deposition of unit 30B at ca. 2 ka. Evidence against the occurrence of a separate event horizon at the base of unit 30B includes: (1) the inconclusive stratigraphic level of the upward terminations of these faults, which may have been obscured by pervasive soil-related cracking of unit 30; and (2) the complete absence of any stratigraphic or structural evidence for significant vertical separations of the unit 40–subunit 30B contact across the faults at meter 9.5 and meter 11. This is in marked contrast to the four surface ruptures that we documented, all of which exhibit significant vertical separations. Moreover, subunit 30B consists of clay that was deposited in a low-energy playa environment, thus making it unlikely that post–unit 40 erosion beveled off any scarps associated with the meter 9.5 and meter 11 faults strands. It is more likely, in our view, that these faults exhibited only minor slip in the most recent event, and are present, but difficult to discern within subunit 30B. Alternatively, many small-displacement faults may not reach all the way to the surface in earthquakes (e.g., Bonilla and Lienkaemper, 1990). Thus, although it is possible that another surface rupture occurred just before event 1, prior to deposition of unit 30B, we think this possibility is unlikely.

Weak evidence for a possible post–event 1 surface rupture comes from east of the main fault, where at least six cracks and small fissures terminate ~0.1–0.2 m below the present ground surface at the base of, or within, unit 20, to the east of the main fault at meter 8 on the southern wall of the northern trench. Unit 20 is lithologically similar to unit 30, and these units may be correlative. However, unit 20 is only exposed on the eastern side of the eastern fault in our northern trench, so this correlation remains somewhat speculative, and the implication of these cracks (which do not appear to have accommodated any slip) remains unclear. If these cracks are younger than event 1, it is possible that they record cracking of the playa surface during strong ground shaking in other earthquakes (i.e., they did not record actual surface rupture on the Calico fault at our trench site).

Event 2

The penultimate surface rupture (event 2) is defined in the northern trench by both upward fault terminations and sedimentary growth of units 40 and 50 across both the eastern and western fault strands into the central trough. As described in detail in the stratigraphic section of the Data Repository material (see footnote 1), units 40 and 50 are the same depositional unit. We distinguish unit 40 as a separate unit based on the development of a weak cambic soil that has been overprinted by a stage II carbonate soil. The depositional unit made up of units 40 and 50 consists predominantly of lacustrine, medium- to coarse-grained sand along with several pale-brown clay subunits that are continuous throughout the northern trench. Within unit 50, the presence of several thin, laterally continuous clay layers allows us to define the geometry of sedimentary growth following event 2, as well as the exact stratigraphic position of the event horizon. Unit 40/50, which onlaps eastward against the fault scarp of event 3 (discussed in the following section), thickens eastward across the western fault strand from a thickness of ~20 cm at meter 26 to a thickness of ~120 cm at meter 12. The parallelism of the lowermost clay subunits within unit 50 suggests that they were deposited on a relatively horizontal substrate. In contrast, fanning of bedding dips for the overlying clay interbeds at meter 10.5–12.0 records onlap during sedimentary growth above a west-facing scarp that developed along the main (eastern) fault during event 2 (Fig. 5). The geometry of these growth strata indicates that the event horizon for the penultimate surface rupture lies near the middle of unit 50. This observation is supported by minor reverse faulting

that occurred during event 2 between meters 21 and 22 along the secondary, western fault strand (Fig. 5; Fig. DR1 [see footnote 1]). This strand displaces the layers below unit 50, as well as the lowest subunits within it, and terminates upward within the upper half of unit 50. Additional evidence in support of event 2 is provided by an upward fault termination at an interbedded clay subunit of unit 50 near meter 24.5 on the southern wall of the northern trench.

Thickening of unit 50 (from a thickness of 20 to a thickness of 120 cm) from meter 26 to meter 12 in the section of the midtrench trough records sedimentary growth of at least 1.0 m following event 2. This stratigraphic growth can be interpreted as a minimum because unit 50 is not exposed east of the main fault at meter 8, and therefore the upper part of unit 50 may have been eroded. Thus, the total vertical separation in event 2 is likely on the order of ~1.0 m.

We dated one sample (081507H) from the bottom of unit 50 and two samples (081507G and 081507F) from the top of the unit, bracketing the occurrence of event 2. The lower sample yielded an age of 5.6 ± 0.4 ka, whereas the upper samples yielded an age of 5.0 ± 0.4 ka. These OSL dates indicate that event 2 occurred between 5.6 ± 0.4 ka and 5.0 ± 0.4 ka.

Event 3

Event 3 is well expressed in the northern trench, where it is defined by the geometry of growth strata, upward fault terminations, and multiple fissure fills within unit 70, a pinkish-brown clay (Fig. 5; Figs. DR1 and DR2 [see footnote 1]). The sedimentary growth during event 3 is most pronounced across the main (eastern) fault zone, where unit 70 thickens westward from ~50 cm at meters 8–11 to >1 m west of meter 11. East of meter 8, unit 70 thins and pinches out eastward by meter 3. The pronounced difference in thickness (0.6 m) of unit 70 between meter 7.5 (east of the main fault) and meter 8.5 (west of the fault) probably reflects erosion of the top of the layer east of the fault. Alternatively, it may reflect strike-slip juxtaposition of a layer of variable along-strike thickness. We think this is less likely, however, because of the near-horizontal morphology of the site, as reflected in the highly planar nature of most of the strata expressed in our trenches. Significant erosion of unit 70 east of the fault is also indicated by the fact that it is overlain directly by the much-younger unit 20. We did not fully expose the unit 70-80 contact across the entire length of the down-dropped, midtrench trough, but unit 70 thins westward from at least 90 cm at its thickest point adjacent to the main (eastern) fault to ~60 cm west of meter 22 across the western fault strand.

Based on the geometry of several fissure fills and the depth of upward fault terminations, event horizon 3 lies within unit 70. Specifically, the event horizon is marked by the top of a fissure fill at meter 24. The fissure extends downward for ~70 cm through unit 80 and is filled with clay from unit 70. Moreover, we were able to trace a weakly developed paleosurface for several meters to the east and west of the fissure on the southern wall of the trench at the same stratigraphic level as the fissure fill. A similar fissure fill was observed in the northern wall of the northern trench at meter 10 at the same stratigraphic level (Fig. DR1 [see footnote 1]). Moreover, the occurrence between meter 8 and meter 3 of multiple fissures within units 80C, 80D, 90, and 100 filled with clay from the lower part of unit 70 suggests that the lower part of unit 70 was at the ground surface during event 3. A fault between meter 11 and meter 12 also terminates upward at the same stratigraphic level as the top of the fissure fill. Unit 70 does not thicken appreciably across the western fault zone, implying that this fault strand experienced minor slip during event 3.

Two OSL samples (081507E and 081507D) from the bottom of unit 70 and two (081507C and 081507B) from the top of the unit constrain the age of event 3. The lower samples yielded ages of 6.1 ± 0.4 ka and

7.3 ± 0.5 ka, whereas the upper samples yielded ages of 5.4 ± 0.4 ka and 5.6 ± 0.4 ka. These ages indicate that event 3 occurred before 5.4 ± 0.4 ka (or 5.6 ± 0.4 ka) and probably after 6.1 ± 0.4 ka. We suspect that the 7.3 ± 0.5 ka age, which was collected from the same stratigraphic level as the 6.1 ± 0.4 ka age, may be less reliable because this sample exhibited the lowest dose rate of all the samples dated, perhaps resulting in an anomalously old age. Alternatively, if the 7.3 ± 0.5 ka age is valid, then event 3 occurred between 5.4 ± 0.4 ka and 7.3 ± 0.5 ka.

Event 4

Event 4, the oldest event horizon we describe, was only observed in the southern trench, where slightly slower sediment accumulation rates allowed us to expose deeper stratigraphic levels (Fig. 4C; Fig. DR2 [see footnote 1]). The event is defined by geometry of growth strata and upward fault terminations. Specifically, if we assume that unit 70, which contains the event 3 horizon in the northern trench, was located near the present ground surface to the east of the main strand in the southern trench (i.e., above unit 90 on the east side of the fault), as seems likely, then the total event 4 vertical separation is ~1.5 m across the main strand between meter 3 and meter 4 in the southern trench. The large minimum vertical separation across the top of unit 90 suggests that event 4 was a relatively large-displacement event. Event 4 is also defined by two fault strands that terminate upward within unit 80D (at meter 3 and meter 4). Moreover, unit 80D, which developed above unit 90, thins eastward against a preexisting scarp that ruptured the top of unit 90 or the lower part of unit 80D. We interpret this as possible evidence for an older event, although this scarp could also have formed during event 4. The overlying unit 80C pinches out against the west-facing scarp formed during event 4. Unit 80A does not change thickness within the trench exposure west of the fault, suggesting that post–event 4 deposition of unit 80C and the upper part of unit 80D had filled in the down-dropped area to the west of the fault and reestablished a near-horizontal surface. These observations indicate the occurrence of at least one surface rupture (i.e., event 4) either during or immediately after the latter stages of deposition of unit 80D.

One OSL sample (081407A) from the top of unit 90 in the southern trench, and two samples (081507E and 081507D) from the bottom of unit 70 in the northern trench, bracket the age of event 4. The sample from unit 90 yielded an age of 8.4 ± 0.7 ka, whereas the two unit 70 samples yielded ages of 6.1 ± 0.4 ka and 7.3 ± 0.5 ka. These three ages indicate that event 4 occurred before 6.1 ± 0.4 ka (or less likely 7.3 ± 0.5 ka) and after 8.4 ± 0.7 ka. As explained earlier, we suspect that the 7.3 ± 0.5 ka date may be less reliable than the 6.1 ± 0.4 ka date because the older sample exhibited the lowest dose rate of all the samples we dated.

MEASUREMENT OF SMALL-SCALE GEOMORPHIC OFFSETS

In addition to our trench study, we also measured displacements in Holocene alluvial deposits exposed over an 8 km length of the fault extending southward from the trench site. We focused on small-scale displacements (<10 m) in an effort to define slip during the past several surface ruptures of most relevance to our paleoseismologic results. Measured displacements at 16 different locations include horizontal and vertical offsets of channels and alluvial-fan surfaces that range from 1.1 ± 0.2 m to 8.7 $^{+2.3}/_{-4.1}$ m (Fig. 8; Table 2). Several of these offsets are preserved along a releasing bend of the Calico fault. In some cases, only one (horizontal or vertical) component of oblique slip could be measured, and total offset was inferred from the ratio of horizontal to vertical displacements at nearby sites (Fig. 8). Altogether the measured displacements fall into two sets: one set of six, ranging from 4.6 ± 0.7 m to 8.7 $^{+2.3}/_{-4.1}$ m, with an

average of 6.7 ± 3.0 m, and a second set of 10, ranging from 1.1 ± 0.2 m to 3.0 ± 1.0 m, with an average of 2.0 ± 1.0 m. The presence of at least two different sets of displacements is further implied by the total oblique displacement of 2.1 ± 0.7 m at location 14 and 4.5 ± 0.7 m at location 13 (Fig. 8; Table 2). At these adjacent locations, a fault scarp (location 14) is present in an offset channel inset into a displaced alluvial fan (location 13). This observation suggests that the channel was incised after at least one earthquake that offset the alluvial-fan surface, and that a subsequent earthquake offset the channel further.

Although it is possible that multiple earthquake events are represented within each set of displacements, we did not observe evidence for more than two events in the field. We prefer an interpretation of two to three events, where the set of smaller-displacement measurements (1.1–3.0 m) records slip in a single earthquake, despite the variability of these offsets (~1 to ~3 m). Given the overlapping distribution of measurement errors of the smallest set of offsets, this interpretation seems likely, and such along-strike variations in slip at adjacent sites have been noted in surface ruptures on other faults (e.g., McGill and Rubin, 1994).

If we account for an average of 2.0 ± 1.0 m of displacement during the most recent event, the penultimate event had an average slip of ~4.7 ± 2.0 m. Alternatively, the average displacement of 4.7 ± 2.0 m may record slip from two different surface ruptures (events 2 and 3), which our paleoseismic data indicate happened closely spaced in time. The potentially brief interevent time between events 2 and 3 suggests that new geomorphic features (e.g., gullies) may not have had sufficient time to develop between these earthquakes. In such a situation, the offsets in events 2 and 3 would appear as a single geomorphically defined offset. In summary, we interpret the two sets of displacements (2.0 ± 1.0 m and 6.7 ± 3.0 m) to record the most recent two, and possibly three, surface ruptures on the Calico fault south of Newberry Springs. However, because we lack age control for the features that are offset, these displacements should be considered maxima for the most recent two (and likely three) events revealed by our trenching study.

DISCUSSION

The paleoseismologic data described here demonstrate that the Calico fault has ruptured to the surface at least four times over the past ~9 k.y. (Fig. 9). The ages of these surface ruptures strongly support the hypothesis that earthquake recurrence in the Mojave section of the Eastern California shear zone is temporally clustered, as originally proposed by Rockwell et al. (2000). Specifically, the most recent event on the Calico fault occurred after 2 ka, as part of an ongoing cluster of earthquakes in the Eastern California shear zone that has been occurring over the past ~1000–1500 yr. Moreover, we see no evidence for any Calico fault surface ruptures during the pronounced seismic lull documented by Rockwell et al. (2000) between 2 and 5 ka, despite the continuous, well-dated stratigraphy exposed in our trenches for this time interval. The penultimate and antepenultimate events on the Calico fault, at 5.0–5.6 ka and 5.6–6.1 (or 5.6–7.3 ka), respectively, also occurred during a pronounced cluster at 5–6 ka documented for other faults in the Mojave part of the Eastern California shear zone by Rockwell et al. (2000). Thus, the Calico fault ruptured twice during the penultimate Eastern California shear zone cluster. Finally, although the timing of the antepenultimate cluster documented by Rockwell et al. (2000) is only broadly constrained between ca. 7 and 11 ka, with a peak in moment release at ca. 8–9.5 ka, it appears that our event 4 occurred toward the end of the cluster between 7.3 ± 0.5 and 8.4 ± 0.7 (or 6.1 ± 0.4 and 8.4 ± 0.7) ka (Fig. 9).

Evidence for two surface ruptures between 5 ka and 6 ka indicates that the Calico fault can rupture more than once during each cluster. Thus,
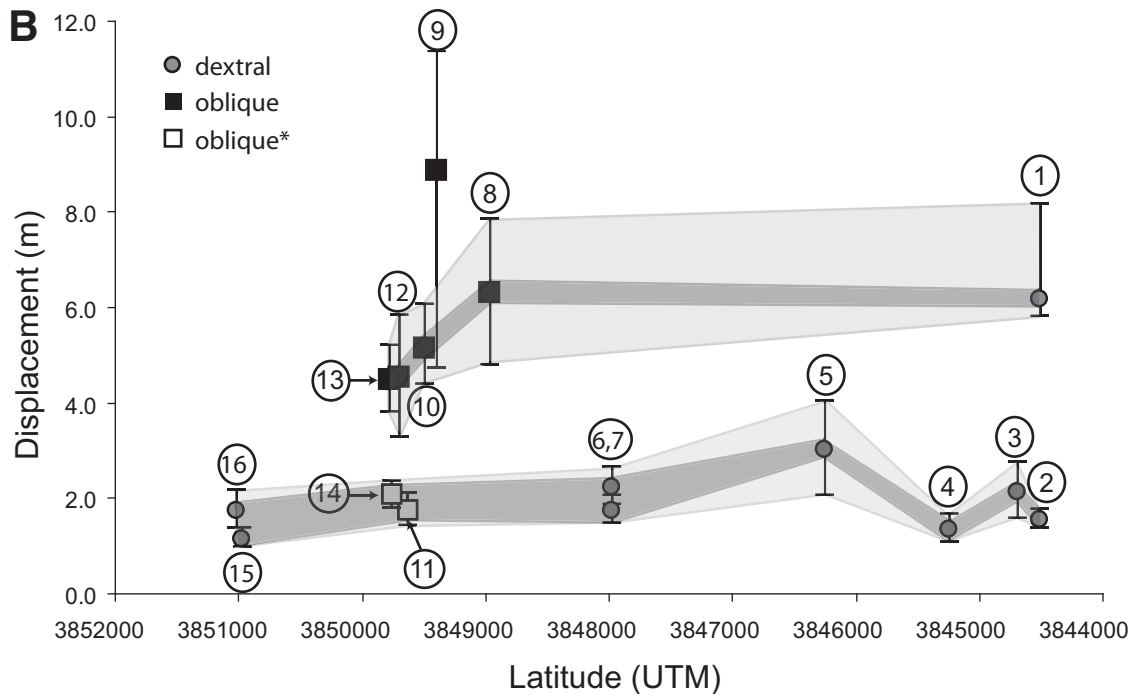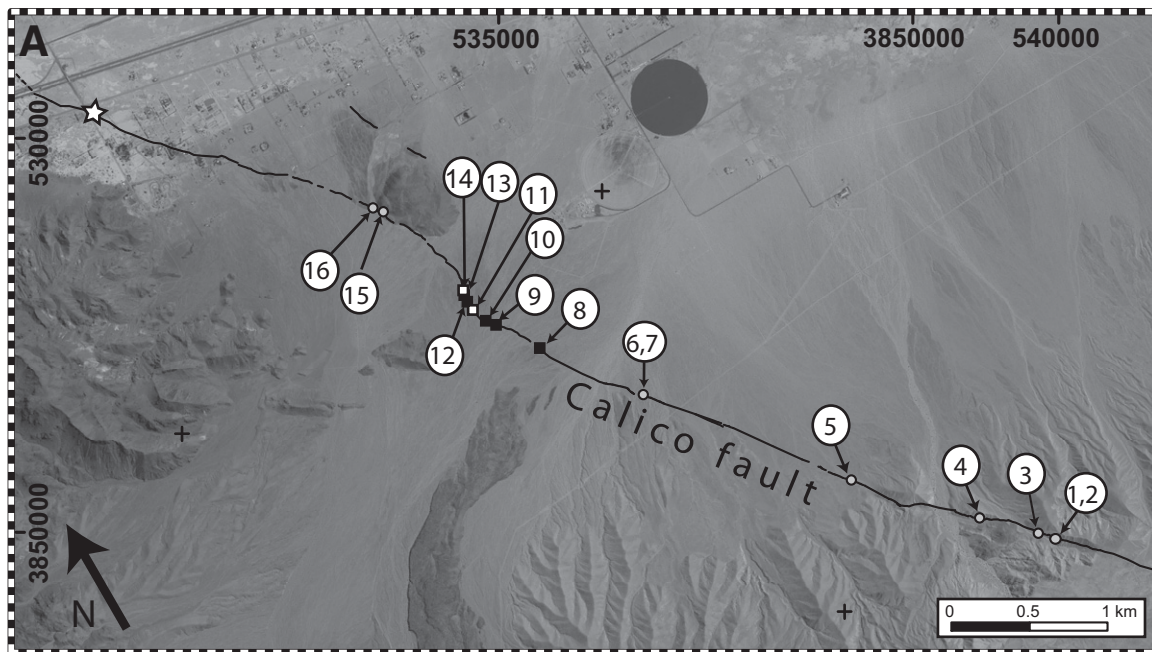
Figure 8. (A) Map showing a part of the northern Calico fault extending southward from our trench site (white star). Circles show the locations of measured horizontal offsets identified along the fault. The solid black squares are locations along a releasing bend of the fault with observed oblique-normal motion. The white squares are locations along the fault where the oblique component of the fault was calculated knowing either the normal or dextral component and assuming a ratio from an adjacent site. (B) Graph showing measured dextral and oblique displacements along the fault. See Table 2 for details.

TABLE 2. SUMMARY OF MEASURED DISPLACEMENTS ALONG THE CALICO FAULT OF
THE EASTERN CALIFORNIA SHEAR ZONE

Location ID	Longitude	Latitude	Displacement* (m)	Error (± m)	Marker/type of displacement	Quality of displacement
1[†]	537209	3844521	6.2	2.0/0.4	Beheaded channel	Very good
2[†]	537209	3844521	1.5	0.2/0.2	Deflected gully	Good
3[†]	537109	3844699	2.1	0.6/0.6	Beheaded channel	Good
4[†]	536592	3845251	1.3	0.3/0.3	Deflected channel	Very good
5[†]	535604	3846264	3.0	1.0/1.0	Deflected channel	Good
6[†]	534285	3847986	1.7	0.3/0.3	Channel thalweg	Good
7[†]	534285	3847986	2.2	0.4/0.4	Channel thalweg	Good
8	533578	3848976	6.0	1.5/1.5	Channel thalweg	Good
8N[†§]	533578	3848976	2.0	0.4/0.4	Alluvial fan	Very good
Total oblique displacement for location 8			**6.3**	**1.6/1.6**		
9	533289	3849405	8.7	2.3/4.1	Channel thalweg	Fair
9N	533279	3849432	2.0	1.0/1.0	Alluvial fan	Very good
Total oblique displacement for location 9			**8.9**	**2.5/4.2**		
10a	533247	3849504	2.4	0.5/0.5	Channel thalweg	Good
10b	533228	3849480	2.2	0.2/0.2	Channel thalweg	Good
Total horizontal offset for location 10			4.6	0.7/0.7		
10Na	533228	3849478	1.0	0.2/0.3	Alluvial fan	Very Good
10Nb	533239	3849486	0.4	0.1/0.1	Alluvial fan	Good
10Nc	533247	3849497	0.9	0.3/0.2	Alluvial fan	Good
Total vertical displacement for location 10			2.3	0.6/0.6		
Total oblique displacement for location 10			**5.1**	**0.9/0.8**		
11	533188	3849683	1.6	0.4/0.4	Channel/alluvial fan	Very good
11N[#]	533188	3849683	0.8	0.3/0.3	Assumed	–
Total oblique displacement for location 11			**1.8**	**0.5/0.5**		
12	533178	3849707	2.3	0.5/0.5	Channel thalweg	Good
12Na	533179	3849698	2.6	0.9/0.9	Alluvial fan	Very good
12Nb	533196	3849705	1.3	0.3/0.3	Alluvial fan	Very good
Total vertical displacement for location 12			3.9	1.2/1.2		
Total oblique displacement for location 12			**4.5**	**1.3/1.3**		
13	533178	3849776	3.5	0.5/0.5	Channel/alluvial fan	Very good
13N	533180	3849789	2.8	0.5/0.5	Alluvial fan	Very good
Total oblique displacement for location 13			**4.5**	**0.7/0.7**		
14**	533176	3849789	1.6	0.5/0.5	Assumed	–
14N	533176	3849772	1.3	0.5/0.5	Alluvial fan	Very good
Total oblique displacement for location 14			**2.1**	**0.7/0.7**		
15	532871	3850980	1.1	0.2/0.2	Deflected channel	Good
16	532835	3851024	1.7	0.4/0.4	Bar edge	Good

*Uncertainties associated with each measurement are based on the maximum and minimum possible dextral offsets of each marker. Uncertainties associated with each normal offset are based on the best-fit slope of the hanging wall and footwall on either side of the fault.

[†]Location along the fault where offset markers were determined in the field with a tape measure. All other measurements were determined by walking the offsets with a field-based differential Global Positioning System and realigning the piercing lines of each marker.

[§]N denotes the location of normal displacement.

[#]Assumed normal displacement is estimated based on a normal:dextral ratio of site 10.

**Assumed dextral displacement is estimated based on a normal:dextral ratio of site 13.
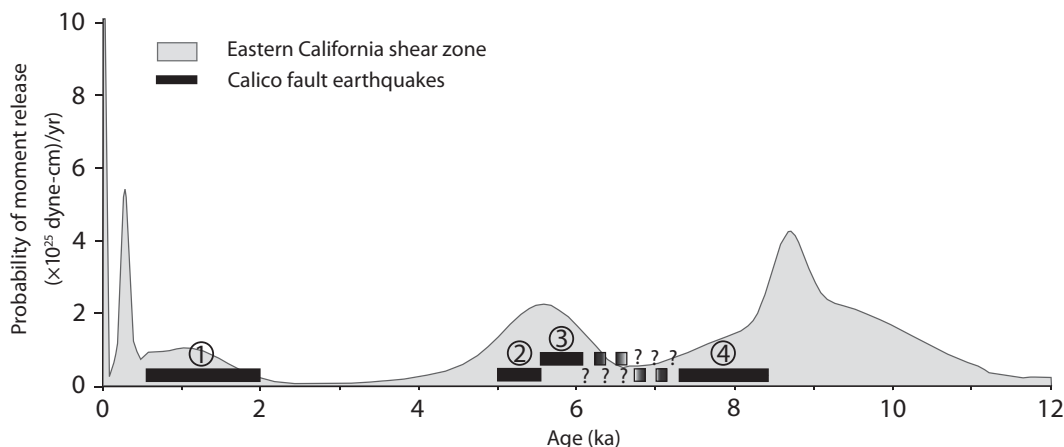
Figure 9. Composition of our paleoearthquake ages (black bars) and compilation of seismic moment release data in the Eastern California shear zone through time (pale gray) from Rockwell et al. (2000). Note the close correspondence of the event ages on the Calico fault (this study) with periods of increased seismic moment release in the region. Circled numbers indicate the four events identified in this study.

although the occurrence of the most recent event after 2 ka suggests that the Calico fault has already ruptured as part of the latest, ongoing earthquake cluster in the Eastern California shear zone, the fault may still be at risk of a near-future earthquake. Furthermore, because no paleoseismic evidence exists for a surface rupture in the past ~600 yr, it is unlikely that the Calico fault ruptured in 1887, as suggested by Bakun (2005). One explanation for these temporally close ruptures is that this section of the fault was an overlap zone between two ruptures on the southern and northern parts of the Calico fault system. Another possibility is that during the 5–6 ka seismic cluster, strain was released in two events on the Calico fault. At this time, we lack sufficient slip-per-event data to test these alternative rupture scenarios. However, the slip-per-event data gathered thus far suggest that ruptures of the Calico fault are similar in size to earthquakes on nearby shear-zone faults (~3 m per earthquake; Rockwell et al., 2000). A higher earthquake frequency thus seems necessary to account for the higher slip rate of the Calico fault when compared to other nearby dextral faults in the Eastern California shear zone.

The vertical separations measured in the paleoseismic trenches may provide some insight into the displacements that occurred during the three most recent earthquakes on the Calico fault. If we assume that the slip vector has remained constant at our study site over the past three events, then the vertical components of the total offsets in each event reflect the relative size of each slip event. The most recent event shows a vertical separation of 0.5 m, suggestive of a small overall displacement. In contrast, the penultimate and antepenultimate surface ruptures exhibit larger vertical separations of ~1 m each, consistent with larger overall displacement in each event. The small vertical separation during the most recent event observed in the trench is consistent with small (~2.0 ± 1.0 m) displacements measured from nearby geomorphic offsets. The remaining geomorphically measured slip (4.7 ± 2.0 m) may be attributed to either one larger penultimate event, consistent with the larger vertical displacement observed in the trench, or it may represent the penultimate and antepenultimate events, which would imply a similar average slip of 2–3 m in each event. Geomorphic offsets on the order of ~2–4 m along the Calico fault imply earthquakes ranging from M_w 7.0 to 7.3 (e.g., Wells and Coppersmith, 1994). The occurrence of larger-displacement events 2 and 3 of the penultimate cluster raises the possibility that the apparently small displacement during the most recent event may be indicative of an ongoing slip deficit.

Interestingly, in addition to the current seismic cluster, the Eastern California shear zone appears to be experiencing a strain transient characterized by geodetic rates (10^0–10^1 yr) that are faster than the long-term geologic rates (10^0–10^6 yr) (Peltzer et al., 2001; Oskin and Iriondo, 2004; Dolan et al., 2007; Oskin et al., 2008). Oskin et al. (2008) documented a cumulative slip rate across the Eastern California shear zone at 35°N of ≤6.2 ± 1.9 mm/yr. In contrast, the rate of right-lateral shear across the entire Mojave Eastern California shear zone measured by global positioning system (GPS) geodesy is 10–14 mm/yr (Savage et al., 1990; Sauber et al., 1994; Dixon et al., 1995; Gan et al., 2000). Thus, there appears to be a significant discrepancy between the short-term rate of elastic strain accumulation measured geodetically and the longer-term geologic slip rates. These observations suggest that the aseismically deforming lower crust and upper mantle beneath the Eastern California shear zone are shearing at a rate that is faster than the long-term average rate documented geologically. Mechanically, this implies that an elevated shear strain rate, likely on a localized, transiently weakened ductile shear zone or set of shear zones, is driving the current cluster of major earthquake activity here (Peltzer et al., 2001; Oskin and Iriondo, 2004; Dolan et al., 2007; Oskin et al., 2008). The mechanisms that permit variable loading rate, and the feedback relationships that may exist among shear-zone strength, fault loading, and

earthquake activity, remain unresolved (Montesí and Hirth, 2003; Dolan et al., 2007; Oskin et al., 2008).

Regardless of the exact mechanism that controls the regional clustering of earthquake activity, or whether or not there is a correlation between earthquake clusters and transiently elevated rates of elastic strain accumulation, the paleoseismologic data from the Calico fault trenches strongly support the notion that seismic moment release within the Eastern California shear zone is highly episodic. Similar examples of spatially and/or temporally clustered seismic moment release have been observed elsewhere on both single faults (e.g., Marco et al., 1996; Stein et al., 1997; Hartleb et al., 2003, 2006; Friedrich et al., 2003; Rockwell et al., 2009b) and regional fault networks (e.g., Dolan and Wald, 1998; Rockwell et al., 2000; Dolan et al., 2007). These observations have fundamentally important implications for probabilistic seismic hazard analysis. Specifically, the increasing body of evidence for clustered earthquake occurrence for at least some, and perhaps many, faults and fault systems (including, for example, the Calico fault) suggests that seismic hazard may be strongly affected by temporally and spatially clustered moment release over epochs much longer than the typical decadal time scale of postseismic relaxation.

CONCLUSIONS

Paleoseismic trenches demonstrate that the past four surface ruptures on the Calico fault (event 1, 0.6 [or 1.1 ka] to 2.0 ka; event 2, 5.0 ka to 5.6 ka; event 3, 5.6 to 6.1 ka (or 7.3 ka); event 4, 6.1 to 7.3 ka [or 8.4 ka]) occurred during clusters of seismic moment release identified earlier on other faults in the Eastern California shear zone as documented by Rockwell et al. (2000). Two different sets of geomorphic displacements (2.0 ± 1.0 m and 4.7 ± 2.0 m) measured in the 8 km south of the trench site suggest that the past two (or three) of the Calico fault earthquakes were large-magnitude (M_w 7.0–7.3) events similar in size to the 1992 M_w 7.3 Landers and 1999 M_w 7.1 Hector Mine earthquakes. Although the most recent event we documented in the trenches occurred after ca. 2 ka, during the ongoing Eastern California shear zone seismic cluster, evidence for two Calico fault surface ruptures during the 5–6 ka cluster suggests the possibility that the Calico fault may rupture more than once during each clustering time period. The evidence of seismic clustering on a regional network of faults provided in this paper adds to a growing body of data suggesting that episodic moment release is common on many faults and fault systems, possibly in response to enhanced loading. Future probabilistic hazard analyses need to account for the possibility of temporally and spatially clustered seismic moment release.

ACKNOWLEDGMENTS

REFERENCES CITED

Adamiec, G., and Aitken, M., 1998, Dose-rate conversion factors: Update: Ancient TL, v. 16, p. 37–50.

Aitken, M.J., 1998, An Introduction to Optical Dating: Oxford, Oxford University Press, 280 p.

Ambraseys, N.N., 1971, Value of historical earthquakes: Nature, v. 232, p. 375–379, doi: 10.1038/232375a0.

Bakun, W., 2005, Historical earthquakes in eastern Southern California, in 2005 Southern California Earthquake Center Annual Meeting Proceedings and Abstracts: Los Angeles, California, Southern California Earthquake Center, v. 15, p. 103–104.

Bonilla, M.G., and Lienkaemper, J.J., 1990, Visibility of fault strands in exploratory trenches and timing of rupture events: Geology, v. 18, p. 153–156, doi: 10.1130/0091-7613(1990)018<0153:VOFSIE>2.3.CO;2.

Crone, A.J., Machette, M.N., Bradley, L.A., and Mahan, S.A., 1997, Late Quaternary surface faulting on the Cheraw fault, southeastern Colorado: U.S. Geological Survey Geologic Investigations Map I-2591, 1 sheet, 7 p., pamphlet.

Dawson, T.E., McGill, S.F., and Rockwell, T.K., 2003, Irregular recurrence of paleoearthquakes along the central Garlock fault near El Paso Peaks, California: Journal of Geophysical Research, v. 108, p. 2356–2385, doi: 10.1029/2001JB001744.

Dixon, T.H., Robaudo, S., Lee, J., and Reheis, M.C., 1995, Constraints on present-day Basin and Range deformation from space geodesy: Tectonics, v. 14, p. 755–772, doi: 10.1029/95TC00931.

Dolan, J.F., and Wald, D., 1998, The 1943–1953 north-central Caribbean earthquake sequence: Active tectonic setting, seismic hazards, and implications for Caribbean–North America plate motions, in Dolan, J.F., and Mann, P., eds., Active Tectonics of the North-Central Caribbean: Geological Society of America Special Paper 326, p. 143–169.

Dolan, J.F., Bowman, D.D., and Sammis, C.G., 2007, Long-range and long-term fault interactions in Southern California: Geology, v. 35, p. 855–858, doi: 10.1130/G23789A.1.

Friedrich, A.M., Wernicke, B.P., Niemi, N.A., Bennett, R.A., and Davis, J.L., 2003, Comparison of geodetic and geologic data from the Wasatch region, Utah, and implications for the spectral character of Earth deformation at periods of 10 to 10 million years: Journal of Geophysical Research, v. 108, no. B4, 2199, doi: 10.1029/2001JB000682.

Gan, W., Svarc, J.L., Savage, J.C., and Prescott, W.H., 2000, Strain accumulation across the Eastern California shear zone at latitude 36°30′N: Journal of Geophysical Research, v. 105, p. 16,229–16,236, doi: 10.1029/2000JB900105.

Hartleb, R.D., Dolan, J.F., Akyuz, H.S., and Yerli, B., 2003, A 2,000 year-long paleoseismologic record of earthquakes along the central North Anatolian fault, from trenches at Alay-urt, Turkey: Bulletin of the Seismological Society of America, v. 93, p. 1935–1954, doi: 10.1785/0120010271.

Hartleb, R.D., Dolan, J.F., Kozaci, O., Serdar Akyuz, H., and Seitz, G.G., 2006, A 2500-yr-long paleoseismologic record of large, infrequent earthquakes on the North Anatolian fault at Cukurcimen, Turkey: Geological Society of America Bulletin, v. 118, no. 7–8, p. 823–840, doi: 10.1130/B25838.1.

Kent, G.M., Babcock, J.M., Driscoll, N.W., Harding, A.J., Dingler, J.A., Seitz, G., Gardner, J.V., Mayer, L.A., Goldman, C.R., Heyvaert, A.C., Richards, R.C., Karlin, R., Morgan, C.W., Gayes, P.T., and Owen, L.A., 2005, 60 k.y. record of extension across the western boundary of the Basin and Range Province: Estimate of slip rates from offset shoreline terraces and a catastrophic slide beneath Lake Tahoe: Geology, v. 33, p. 365–368, doi: 10.1130/G21230.1.

Lee, J., Spencer, J.Q., and Owen, L.A., 2001, Holocene slip rates along the Owens Valley fault, California: Implications for the recent evolution of the Eastern California shear zone: Geology, v. 29, p. 819–822, doi: 10.1130/0091-7613(2001)029<0819:HSRATO>2.0.CO;2.

Machette, M.N., Personius, S.F., and Nelson, A.R., 1992, The Wasatch fault zone, USA: Annales Tectonicae, v. 6, p. 5–39.

Marco, S., Stein, R., and Agnon, A., 1996, Long-term earthquake clustering: A 50,000-year paleoseismic record in the Dead Sea graben: Journal of Geophysical Research, v. 106, p. 4103–4120.

McGill, S.F., and Rubin, C.M., 1994, Variability of surficial slip in the 1992 Landers earthquake; implications for studies of prehistoric ruptures, in Prentice, C.S., Schwartz, D.P., and Yeats, R.S., eds., Proceedings of the Workshop on Paleoseismology: U.S. Geological Survey Open-file Report 94-56, p. 118–120.

Mejdahl, V., 1979, Thermoluminescence dating: Beta attenuation in quartz grains: Archaeometry, v. 21, p. 61–72, doi: 10.1111/j.1475-4754.1979.tb00241.x.

Montési, L.G.J., and Hirth, G., 2003, Grain size evolution and the rheology of ductile shear zones: From laboratory experiments to postseismic creep: Earth and Planetary Science Letters, v. 211, p. 97–110, doi: 10.1016/S0012-821X(03)00196-1.

Murray, A.S., and Wintle, A.G., 2000, Luminescence dating of quartz using an improved single-aliquot regenerative-dose protocol: Radiation Measurements, v. 32, p. 57–73, doi: 10.1016/S1350-4487(99)00253-X.

National Agriculture Imagery Program, 2005, Indiana Spatial Data Portal: Indiana University, http://www.indiana.edu/~gisdata/statewide/05naip.html.

Oskin, M., and Iriondo, A., 2004, Large-magnitude transient strain accumulation on the Blackwater fault, Eastern California shear zone: Geology, v. 32, p. 313–316, doi: 10.1130/G20223.1.

Oskin, M., Perg, L., Blumentritt, D., Mukhopadhyay, S., and Iriondo, A., 2007, Slip rate of the Calico fault: Implications for geologic versus geodetic rate discrepancy in the Eastern California shear zone: Journal of Geophysical Research, v. 112, B03402, doi: 10.1029/2006JB004451.

Oskin, M., Perg, L., Shelef, E., Strane, M., Gurney, E., Singer, B., and Zhang, X., 2008, Elevated shear zone loading rate during an earthquake cluster in eastern California: Geology, v. 36, p. 507–510, doi: 10.1130/G24814A.1.

Owen, L.A., Cunningham, W.D., Richards, B., Rhodes, E.J., Windley, B.F., Dornjamjaa, D., and Badamgarav, J., 1999, Timing of formation of forebergs in the northeastern Gobi Altai, Mongolia: Implications for estimating mountain uplift rates and earthquake recurrence intervals: Journal of the Geological Society, v. 156, no. 3, p. 457–464, doi: 10.1144/gsjgs.156.3.0457.

Peltzer, G., Crampe, F., Hensley, S., and Rosen, P., 2001, Transient strain accumulation and fault interaction in the Eastern California shear zone: Geology, v. 29, p. 975–978, doi: 10.1130/0091-7613(2001)029<0975:TSAAFI>2.0.CO;2.

Prescott, J.R., and Hutton, J.T., 1994, Cosmic ray contributions to dose rates for luminescence and ESR dating: Large depths and long-term time variations: Radiation Measurements, v. 23, p. 497–500, doi: 10.1016/1350-4487(94)90086-8.

Rockwell, T.K., Lindvall, S., Herzberg, M., Murbach, D., Dawson, T., and Berger, G., 2000, Paleoseismology of the Johnson Valley, Kickapoo, and Homestead Valley faults: Clustering of earthquakes in the Eastern California shear zone: Bulletin of the Seismological Society of America, v. 90, p. 1200–1236, doi: 10.1785/0119990023.

Rockwell, T., Fonseca, J., Madden, C., Dawson, T., Owen, L.A., Vilanova, S., and Figueiredo, P., 2009a, Palaeoseismology of the Vilariça segment of the Manteigas-Bragança fault in northeastern Portugal, in Reicherter, K., Michetti, A.M., and Silva, P.G., eds., Palaeoseismology: Historical and Prehistorical Records of Earthquake Ground Effects for Seismic Hazard Assessment: Geological Society, London, Special Publication 316, p. 237–258, doi: 10.1144/SP316.15.

Rockwell, T.K., Ragona, D., Seitz, G., Langridge, R., Aksoy, M.E., Ucarkus, G., Ferry, M., Meltzner, A.J., Klinger, Y., Meghraoui, M., Satir, D., Barka, A., and Akbalik, B., 2009b, Palaeoseismology of the North Anatolian fault near the Marmara Sea: Implications for fault segmentation and seismic hazard, in Reicherter, K., Michetti, A.M., and Silva, P.G., eds., Palaeoseismology: Historical and Prehistorical Records of Earthquake Ground Effects for Seismic Hazard Assessment: Geological Society, London, Special Publication 316, p. 31–54, doi: 10.1144/SP316.3.

Sauber, J., Thatcher, W., Solomon, S.C., and Lisowski, M., 1994, Geodetic slip rate for the Eastern California shear zone and the recurrence time of Mojave Desert earthquakes: Nature, v. 367, p. 264–266, doi: 10.1038/367264a0.

Savage, J.C., Lisowski, M., and Prescott, W.H., 1990, An apparent shear zone trending north northwest across the Mojave Desert into Owens Valley, eastern California: Geophysical Research Letters, v. 17, p. 2113–2116, doi: 10.1029/GL017i012p02113.

Stein, R.S., Barka, A.A., and Dieterich, J.H., 1997, Progressive failure on the North Anatolian fault since 1939 by earthquake stress triggering: Geophysical Journal International, v. 128, p. 594–604, doi: 10.1111/j.1365-246X.1997.tb05321.x.

Wallinga, J., 2002, Optically stimulated luminescence dating of fluvial deposits: A review: Boreas, v. 31, p. 303–322, doi: 10.1080/030094802320942536.

Washburn, Z., Arrowsmith, J.R., Forman, S.L., Cowgill, E., Xiaofeng, W., Yueqiao, Z., and Zhengle, C., 2001, Late Holocene earthquake history of the central Altyn Tagh fault, China: Geology, v. 29, p. 1051–1054, doi: 10.1130/0091-7613(2001)029<1051:LHEHOT>2.0.CO;2.

Weldon, R., Fumal, T., and Biasi, G., 2004, Wrightwood and the earthquake cycle: What a long recurrence record tells us about how faults work: GSA Today, v. 14, no. 9, doi: 10.1130/1052-5173(2004)014<4:WATECW>2.0.CO;2.

Wells, D.L., and Coppersmith, K.J., 1994, New empirical relationships among magnitude, rupture length, rupture width, rupture area, and surface displacement: Bulletin of the Seismological Society of America, v. 84, no. 4, p. 974–1002.

Wesnousky, S.G., Barron, A.D., Briggs, R.W., Caskey, S.J., Kumar, S., and Owen, L., 2005, Paleoseismic transect across the northern Great Basin: Journal of Geophysical Research, v. 110, B05408, doi: 10.1029/2004JB003283.